JOURNAL OF OPTOELECTRONICS AND ADVANCED MATERIALS Vol. 9, No. 3, March 2007, p. 721 - 724

Electron Spin Resonance analysis of Si nanocrystals embedded in a SiO_2 matrix

M. JIVANESCU[*], A. STESMANS, S. GODEFROO, M. ZACHARIAS[a]
Department of Physics, University of Leuven, Celestijnenlaan 200 D, B-3001 Leuven, Belgium
INPAC-Institute for Nanoscale Physics and Chemistry, University of Leuven, Belgium
[a]Institute of Microstructure Physics, Weinberg 2, 06120 Halle, Germany

Low-temperature electron spin resonance (ESR) has been used to analyze Si nanoparticles embedded in a SiO_2 matrix, formed by thermal annealing of SiO/SiO_2 superlattices. These structures exhibit an intense broad photoluminescence (PL) peak, the origin of which is still intensely investigated. Both quantum confinement and influence of defects have been proposed as possible origin. In an attempt to further insight, we have performed extensive ESR measurements with the view to address this controversial matter from the defect side. In initial work, the various types of naturally occurring point defects were categorized and identified, both in the as received state and after appropriate photon irradiation. Knowledge of the detailed atomic nature of the revealed defects in connection with previous work on Si/SiO_2 enables us to trace down the exact location of the defects, which is a key point as the centers may pertain to various locations within the SiO/SiO_2 superstructures with embedded Si nanoparticles. As a general finding, it appears that the phase-separated SiO/SiO_2 superstructures exhibit a substantial density of inherent point defects (P_b type defects, D, EX, and E' centers), the potential effect of which on the PL behavior is unclear up to now.

(Received November 15, 2006; accepted December 21, 2006)

Keywords: Si nanocrystals, ESR, SiO_2 matrix

1. Introduction

The optoelectronic and semiconductor industry is majorly based on silicon technology. With respect to optical activity, extensive research has been conducted on porous silicon, with promising results [1]. Yet, a main problem is its fragility for standard industrial manipulation and the high reactivity of the surface that cannot be passivated using known technologies [2] without having an impact on the optical and electrical properties. So, other directions have been investigated. Part of the research has taken the route of the Si nanoparticles embedded in an oxide matrix, SiO_2 in this case. Such structures exhibit an interesting photoluminescence property, which has evoked much interest for potential applications [3]. Various methods are in use to obtain this type of structure. Yet there still exist general major obstacles such as the size and density control of the nanocrystals or the fact that they may ‘touch’ each other, limiting the efficiency of the luminescence in the visible range attributed to nonradiative processes at the particle boundaries.

In this work, first high-sensitivity ESR analysis is applied to nano-Si particles/SiO_2 superstructures fabricated by the SiO/SiO_2 superlattice approach with the intent, in a first ansatz, to reveal, categorize, and quantify occurring paramagnetic defects. Based on the knowledge of the atomic nature, we asses the location of these centers, i.e., with what specific feature of the structure the separate types of defects are connected with, which may be used as a platform for further analysis of the potential influence of defects on the observed photoluminescence.

2. Experimental details

Rather recently, a new method has been proposed [3] to prepare structures composed of Si nanoparticles embedded in SiO_2 based thermal annealing of SiO/SiO_2 superlattices.

For the current work, alternate SiO/SiO_2 layers of 2 and respectively 4 nm thick are deposited onto (100) p-Si wafers by reactive evaporation of SiO powders alternatively in vacuum or oxygen ambient of well controlled pressure (typically ~ 10^{-4} mbar). After high temperature (~1100°C; N_2) annealing, phase separation occurred, resulting in Si nanoparticles of approximately 2 nm diameter formed between ~ 4 nm thick SiO_2 layers [3]. The formation of the Si nanoparticles, their diameter, and the thickness of the SiO_2 layers have been analyzed by cross-section TEM and electron microscope measurements [3]. The number of SiO/SiO_2 periods applied was 45, resulting in a total thickness of the superstructure of 270 nm. For ESR purposes, slices of 2x9 mm^2 main face were cut. After some thinning down and selective elimination (wet chemical etching) of the cutting damage and back interface, maximally 4 slices could be stacked in one ESR sample. This makes the total sample surface we probed to be ~0.72 cm^2, which by Si/SiO_2 ESR standards is not very large (small number of defects), delimiting detectivity and achievable signal-to-noise ratio.

Conventional first order absorption-derivative (dP_μ/dB, where P_μ and B represent the incident microwave power and applied magnetic field, respectively) ESR is measured using a K-band spectrometer operating at a

frequency of ~ 20.5 GHz, equipped with a TE_{011} cavity. The sensitivity of the spectrometer increases with decreasing the temperature, but at the same time, signal saturation increases. For reasons of sensitivity, all the measurements were taken at 4.2 K. The measurements were performed with the amplitude of the applied sinusoidal modulation of the magnetic field (~ 100 kHz) and incident microwave power properly adjusted so that the measured signals were not visibly distorted (no overmodulation and/or saturation). In order to improve the signal-to-noise ratio for each spectrum we typically accumulated 100 scans.

For the sake of ESR signal intensity and g factor calibration, a Si:P marker sample (spin S = 1/2; g (4.2 K) = 1.99869 ± 0.00002) was identically co-mounted with the superstructure sample for each measurement. To get the absolute values of the defect densities we compared for each one the double numerical integration of its detected derivative-absorption spectrum with that of the marker, both recorded in the same trace. Generally, measurements were carried out with the applied magnetic field $\vec{B} \parallel \vec{n}$, the (100)Si substrate normal. The signal anisotropy was checked by varying the angle (φ_B) $\vec{B}$ makes with the [100] interface normal $\vec{n}$.

The samples were sequentially subjected to various irradiation treatments in the attempt to find out whether point defects can have an influence on the strong PL reported [3]. A major goal is to compare and investigate the influence of illumination on the density of ESR-active point defects present in the superstructure.

To establish a reference for the observed defects prior to any illumination, we first measured by ESR the sample in the as-received state, so, without any supplementary treatment, apart from the ones done by the manufacturers. In an attempt to emulate the effect the laser used during PL measurements has on the sample we used different light sources, in combination with methods to spread the emitting light evenly over the entire sample area in order to maximize ESR sensitivity.

A first optical step implied illumination using a He-Cd laser with an output wavelength of approximately 325 nm (3.81 eV) for 22.5 h, in combination with a defocusing lens. Because of the low power of the He-Cd laser (15 mW) that decreases considerably at the sample surface when the beam is defocused, the illumination is insufficient to simulate *focused* laser beam impact. That is why we applied in a second step illumination for 71 h from a 150 W (electrical power) xenon arc lamp arrangement with an interference filter passing wavelengths of 362 ± 20 nm.

As an additional check whether there will be some significant amount of H present in the sample, we illuminated with photons (UV) that would crack-off bonded H, to maximally determine the number of point defect precursors present. For this we removed the filter from the 150 W xenon arc lamp, thus obtaining at the sample the lamp's full (unfiltered) UV spectrum (180-700 nm) and applied it for another 11 h. We also subjected the samples to higher energy light illumination obtained from a VUV krypton resonance discharge lamp, with the spectrum centered at 10.02 eV for 10 min, covering the entire surface of all the slices. The problem with the higher energy of the irradiating light is that its penetration depth is shallow (~ 10 nm).

One sample was subjected successively to all four treatments described above. The ESR measurements were carried out on the as received sample and after each separate illumination step to reveal possible connections with the kind of point defects and densities turned on (ESR activated), and the type of illumination applied.

3. Results and analysis

Fig. 1 shows representative ESR spectra measured on the as received sample (top curve), and after subsequent filtered (362 nm) xenon lamp (curve (b)) and full xenon lamp [curve (c)] illumination. We do not show any spectrum corresponding to the He-Cd laser illumination because there is no visible change compared to the as received sample. One cause can be the insufficient power of the laser to affect defects observably. Also, due to the fact that there is no noticeable difference in the ESR signals between the full UV xenon lamp and VUV irradiated samples we neither show spectra observed after the latter irradiation.

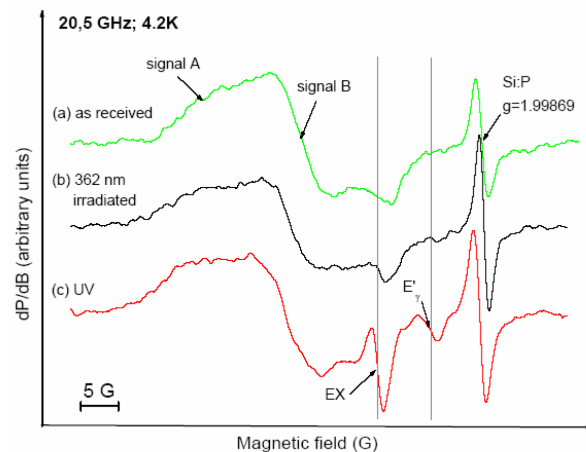

Fig. 1. Absorption-derivative K-band ESR spectra observed at 4.2 K under similar spectroscopical settings on Si-nanoparticles/SiO_2 superstructures in the (a) as received state, (b) after xenon arc lamp illumination at ~362 nm using an interference filter and (c) after full spectrum xenon arc lamp irradiation. The signal at g=1.99869 stems from a co-mounted Si:P marker sample.

As exposed by Fig. 1(a), for the as received sample, two broad overlapping signals are observed, denoted A and B, of comparable intensity, at zero crossing g value g_c ≈ 2.0057. From previous knowledge from ESR investigations on Si/SiO_2 structures, the kind of g_c value and signal width would point to P_b-type defects and/or D centers. The P_b type centers are archetype Si/SiO_2 interface

defects located right at the Si/SiO_2 interface, and in fact, are heralds of the presence of such interface in the sample. Generally, three types have been isolated [4]. Specifically, these are the P_b defects (identified as interfacial $Si_3\equiv Si^\bullet$) [5, 6] at the (111) Si/SiO_2 interface, and the P_{b0} and P_{b1} centers [4, 5, 7]at the (100) Si/SiO_2 interface. All three types are Si dangling bond type centers, which, very importantly, are well in registry with the crystallinity of the Si substrate, that is, the ESR spectra at a macroscopic Si/SiO_2 interface shows very specific anisotropy with varying orientation of $\vec{B}$. As to the D centers, typically of $g \approx 2.0055$, these are also $Si_3\equiv Si^\bullet$ type centers, but located in a disordered Si surrounding. [8]

In this respect, a further pertinent observation is that no variation, within experimental error, of the signal(s) position or intensity is observed with varying φ_B. This would tell us two facts: First, we cannot discern, against the background of the signals observed, the P_b - type signals definitively present at the macroscopic (100) Si/SiO_2 interface. But in the case of the (100) p-Si wafer used as a substrate for such a small area (~0.72 cm^2) of Si/SiO_2 interface, the expected regular P_{b0} and P_{b1} interface point defects is less than 5 % of the sum of the densities of the A and B signals [see, e.g., Ref 9], so the former signal would not be discernable.

Second, if signals A/B originate from P_b-type interface defects, they must stem from the Si nanoparticles/SiO_2 interfaces, bordered by facets of various orientations. The overall signal observed would then be some kind of powder pattern of P_b-type defects.

In trying to simulate the A/B spectrum, we considered various scenarios. Two were successful: In a first case we obtain good overall fitting by combining the D signal with the P_b powder pattern; in the second case, the powder patterns of the P_{b0} and P_{b1} point defects were combined. So, with respect to the Si nanoparticles/Si nanocrystals, depending on the developed orientation of the surface, we can have P_b point defects in the case of (111)Si [5] and (110)Si [10] facets, and P_{b0} and P_{b1} in the case of (100)Si [4, 5, 9] facets.

Somewhat disappointingly, the attained fitting quality in both cases is similar and we cannot quite discriminate within experimental accuracy which situation would apply. If we consider the simulation based on the P_b and D centers to be the likely one, that would definitely imply that part of the Si nanoparticles system is in the amorphous state or that the surface of the nanocrystals have a (very) thin disordered shell [11]. The inferred density of the P_b -type point defects of (3.5 ± 26 %) x 10^{13} cm^{-2} is very close to the density of the D centers of (3.9 ± 20%) x 10^{13} cm^{-2}. If taking an average diameter of 2 nm for the Si nanoparticles we find in average one P_b center or one D center for each 3.8 Si nanoparticles. If only focusing on P_b-type centers and taking into account that P_b point defects pertain only to the Si/SiO_2 interfaces, the P_b -type defect density for the Si nanoparticles would be 1 x 10^{12} cm^{-2}. Compared to the typical value encountered for the thermally grown microscopic (111) and (100)Si/SiO_2 interfaces in the range (1 - 5) x 10^{12} cm^{-2} [9, 12], it would mean that the interfaces of both systems are comparable.

The Si nanoparticles are likely bordered by a mix of nanosized facets of different Si crystalline planes (e.g. (100), (111), or (110)). However, since on the one hand distinction between the P_b and P_{b0} defects cannot be made, and on the other hand, discrimination in fitting between the $P_{b(0)}$/D and P_{b0}/P_{b1} case cannot be made, we cannot yet come to a clear conclusion as to what kind of facets would actually be involved.

As to the behavior of those two signals (A and B) as a function of kind of irradiation type and time applied, we can conclude that there is no distinct variation within experimental error of ±30 %. The constant values give an extra proof that there is no significant hydrogen passivation of the P_b [13, 14] and D centers, in agreement with the final phase-separating annealing step of 1100°C in N_2 applied by the manufacturers. The sample is H lean.

In Figure 1(b) the E'_γ defect (generic entity $O_3\equiv Si^\bullet$), an amorphous SiO_2-specific defect [15], starts to become visible and in Figure 1 (c) increases drastically. The increase can be correlated with the exposure to UV and VUV.

In Figure 1(c) another SiO_2 specific defect, called EX, is present [16]. It is modeled as an entity composed of a cluster of four oxygen atoms, each of them back bonded to 3 Si atoms, with one electron delocalized over the oxygen atoms, and one O–O bend bond. Both SiO_2-related defects, i.e., E' and EX, are strongly activated by high energy irradiation [17]. This is even true for VUV irradiation which would penetrate only a small fraction of the sample's depth, compared with UV that goes all the way through the superstructure. Since both of the defects are pertaining only to SiO_2 matrix we will not discuss these in the present article.

4. Conclusions

The studied Si nanoparticles/SiO_2 superstructures in the as-annealed crystallized state, without any optical excitation applied, are found to *inherently* exhibit a significant amount of ESR active point defects. This situation stayed unaltered after high-energy photon irradiation (UV, VUV), indicating there appears to be no measurable hydrogen passivation, in compliance with sample preparation. From the ESR measurements, it is obtained that the density of the Si/SiO_2 interface-specific defects, corresponding to the Si nanoparticles/SiO_2 interfaces is comparable to that of the regular microscopic Si/SiO_2 interface.

However, as a result of photonic excitation, it is found that UV and VUV irradiations do generate (activate) ESR-active centers, namely E' and EX, but these point defects are associated with the $SiO_{2(x)}$ matrix and are not discussed in detail here.

All the defects present in the sample, but especially the high density of P_b and D centers, may play a key role in the structure's electronic response and the possible influence of these should be considered for the PL behavior of the envisioned superstructures. Detailed comparison with PL measurement is underway.

References

[1] Z. Yamani, A. Alaql, J. Therrien, O. Nayfeh, M. Nayfeh, Appl. Phys. Lett. **74**, 3483 (1999).

[2] E. J. Nemanick, P. T. Hurley, L. J. Webb, D. W. Knapp, D. J. Michalak, B. S. Brunschwig, N. S. Lewis, J. Phys. Chem. B **110,** 14770 (2006).

[3] M. Zacharias, J. Heitmann, R. Scholz, U. Kahler, M. Schmidt, J. Blasing, Appl. Phys. Lett. **80**, 661 (2002).

[4] See, e.g., E. H. Poindexter, Semicond. Sci. Technol. **4**, 961 (1989); D. Pierreux, A. Stesmans, Phys. Rev. **B66**, 165 (2002); A. Stesmans, V. V. Afanas'ev, J. Appl. Phys. **83**, 2449 (1998).

[5] E. H. Poindexter, P. Caplan, B. Deal, R. Razouk, J. Appl. Phys. **52**, 879 (1981)

[6] K. L. Brower, Appl. Phys. Lett. **43**, 1111 (1983)

[7] R. Helms, E. Poindexter, Rep. Prog. Phys. **57**, 791 (1994)

[8] See, e.g., P. C. Taylor, in Semiconductors and Semimetals, Vol 21C, edited by J. I. Pankove (Academic, N.Y., 1984), p. 99; and references therein.

[9] A. Stesmans, V. V. Afanas'ev, J. Vac. Sci. Technol. **B16**, 3108 (1998)

[10] E. H. Poindexter, P. J. Caplan, Electrochem. Soc. Proc. **88**, 299 (1988)

[11] Zimina, St. Eisebitt, W. Eberhardt, J. Heitmann, M. Zacharias, Appl. Phys. Lett. 88 (2006) 163103.)

[12] W. Futako, M. Mizuochi, S. Yamasaki, Phys. Rev. Lett. **92**, 105505 (2004).

[13] K. L. Brower, Phys. Rev. 9657 (1988); Phys. Rev. **B42**, 3444 (1990).

[14] A. Stesmans, J. Appl. Phys. **88**, 489 (2000).

[15] D. L. Griscom, in Glass: Science and Technology Vol 4B, edited by D. R. Uhlmannn and N. J. Kreidl (academic Press, N.Y., 1990), p. 151

[16] A. Stesmans, F. Scheerlinck, Phys. Rev. **B50**, 5204 (1994).

[17] T. E. Tsai, D. L. Griscom, Phys. Rev. Lett. **61**, 444 (1988).

*Corresponding author: mihaela.jivanescu@fys.kuleuven.be